

Hardness, Microstructure and Corrosion Behaviour of WC-9Co-4Cr+TiC Reinforced Stainless Steel

A P I Popoola*

Department of Chemical, Metallurgical and Materials Engineering, Tshwane University of Technology, P.M.B. X680, Pretoria, South Africa, 0001.

*E-mail: PopoolaAPI@tut.ac.za;

Received: 3 November 2013 / *Accepted:* 10 December 2013 / *Published:* 5 January 2014

WC-9Co-4Cr+TiC particles reinforced 304L austenitic stainless steel (ASS) matrix composites (MMCs) were fabricated by laser melt injection (LMI) technique. The morphologies and microstructures of the composite coatings were investigated using optical (OPM) and high resolution scanning electron microscopes (SEM). The constituent phases and elements were observed using x-ray diffraction (XRD) and energy dispersive spectrometry (EDS) respectively. The microhardness measurements were carried out using the Vickers tester. Experimental results revealed that the MMCs layers were crack free but with irregular distribution of TiC-aggregates. The top of the alloyed zone comprises of undissolved big and round clusters of WC as well as faceted dendrites. The middle and bottom parts of composite layer exhibit regular microstructure with finely distributed WC dendrites. A significant increase in microhardness of the stainless steel matrix was achieved, from 236 to 1016 $H_{v0.1}$. The corrosion properties of the WC-9Co-4Cr+TiC reinforced stainless steel were the most improved compared with other MMCs studied.

Keywords: Laser melt injection, metal matrix composites: WC-9Co-Cr; TiC; corrosion, microhardness

1. INTRODUCTION

The 304L austenitic stainless steel material (304L ASS) has a wide range of industrial applications, and this has provoked lots of researches aimed at enhancing the properties of this material [1]. Technological advancements are funded by different national governments and thus increase daily. This has however propelled the application of metallic alloys and components in more aggressive industrial conditions. The scope of materials that can withstand these conditions is at present very restricted and often considerably more expensive. Surface engineering is the key to the problem.

Surface engineering technologies in recent years have been developed to improve the properties of stainless steels, aluminium, magnesium etc. without influencing their bulk properties. Such techniques include laser, thermal spray, electroplating, vapour deposition, ion implantation and sol-gel. Among all these techniques, laser applications are state of the art techniques that enable extended application of materials. Lasers have been frequently used to fabricate metal matrix composites (MMCs) on stainless steels. Metal matrix composites (MMCs) are materials that consist of a matrix which is the base material with a second phase that has been synthetically introduced.

Lasers can produce rapidly solidified zone, because the process is carried out at very high temperatures which lead to rapid melting and cooling. The microstructure, phases and the distribution of the reinforced powders are modified and sometimes homogenized [1]. This modification is however dependent on the processing parameters employed. Several hardfacing particles such as TiC, WC etc. have been injected to the melt pool of stainless steel alloys [2–5]. 304L ASS material display good corrosion and oxidation resistances properties in most environments. It is an added advantage if any material exhibit good surface properties (corrosion, hardness, wear, fatigue and etc). However, 304L ASS exhibits poor hardness property which leads to poor tribological and fatigue resistant properties (interrelated); these limitations affect the industrial usage of this material. By adding a controlled amount of these powders, carbide phases can be precipitated during chemical reactions occurring within the melt pool during laser processing. This leads to high hardness and consequently the improvement of other properties that depends on the hardness like the wear and the fatigue resistances.

However, the deposition of reinforcement particles to enhance properties could considerably deteriorate the corrosion behaviour of metallic materials. Between a metallic material and its service environment, physicochemical reactions leading to the damage of its surface properties (corrosion) can take place; resulting into failure and probable plant shutdowns. Corrosion is very deleterious and as such this phenomenon should be prevented. Secondly, corrosion reactions can be initiated because of the presence of defects and heterogeneities in the coatings formed owing to the presence of particulates, precipitates (carbides/intermetallic) typically formed as reaction products in the melt pool during laser processing [6]. Microsegregation also depreciates the corrosion properties of steel alloyed surfaces. Full blown corrosion reactions often take place at the different interfaces within the coating. Wu et al. [7] studied the influence of TiC particle addition on 304 stainless steels prepared using a vacuum medium frequency induction melting furnace and the corrosion behaviour was compared in 5 wt.% HCl solution. It was reported that addition of TiC particles to 304SS resulted in no rapid pit propagation but maintained a high corrosion rate in the whole immersion time. The corrosion behaviour of TiC particles reinforced Mg-Al alloy in 3.5% NaCl solution was also reported by Falcon et al. [8], evidence of galvanic effects was found which increased the composite corrosion rate between the matrix and the TiC particles.

There is an obvious need for proper optimization of the laser processing parameters and preference of carbide reinforcement. The aim of this study will be to investigate the possibility of improved surface dependent properties; increase the hardness property which is related to its wear and fatigue resistances and at the same confirm that the corrosion resistance has not be altered adversely but rather sustained/enhanced. Laser melt injection (LMI) technique will be used to incorporate carbides onto the matrix 304L ASS. Since corrosion properties is highly sensitive to surface

inhomogeneity, an attempt will be made to eliminate this by the use of laser, this should mitigate against the initiation of corrosion reactions while the hardness of the material is being modified. This paper will also look into the microstructural characterization of the developed 304L ASS MMCs. The influence of laser processing parameters employed on the properties of the developed MMCs will be studied as well.

2. EXPERIMENTAL DETAILS

In this study, 304L austenitic stainless steel was the metal substrate. The chemical composition of the stainless steel sample is shown in Table 1. Pure WC-9Co-4Cr and TiC powders supplied by Weartech (Pty) Ltd were used as the reinforcement carbides. The as-received powders as shown in Fig. 1 were characterized for particle size distribution and morphology. The particle size distribution was analyzed using a Malvern Mastersizer 2000 particle size analyzer (Microscientific) with water as a carrier fluid. WC-9Co-4Cr particles are fine sized (agglomerated and sintered) with average particle size results of 26 μm while TiC particle morphology is coarse (sintered and crushed) with average particle size of 83 μm. The powders were mixed in the ratio 70:30 (WC-9Co-4Cr:TiC) weight percent in a dry environment at room temperature for 8 hours using the Turbula mixer.

Table 1. Nominal chemical composition of 304L austenitic stainless steel

Sample	Cr	Ni	Mo	Si	Mn	N	Cu	S	P	C	Fe
Percentage composition (%)											
304L	18.7	9.2	-	0.45	1.50	-	-	0.001	0.027	0.02	Bal

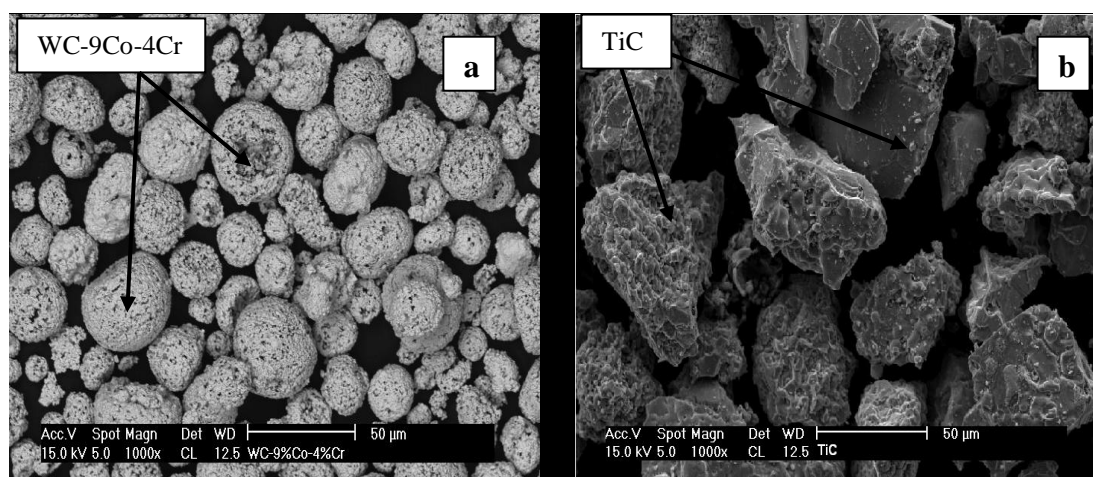


Figure 1. SEM image of (a) WC-9Co-4Cr (b) TiC reinforcing materials

Prior to injection, the substrates were sandblasted before exposure to laser beam to enhance the absorption of the laser beam radiation and basically clean their surfaces [9-10]. LMI experiment was

carried out using a 4.4 kW Rofin Sinar continuous wave Nd: YAG laser equipped with a fibre optic beam delivery system. The powders were fed laterally using a commercial powder feeder instrument equipped with a flow balance to control the powder feed rate. During the LMI process, the laser beam with power of 2.0 kW, scan speed of between 0.6 to 1.2 m/min and 3 mm beam diameter was used to create a melt pool of single track on the surface of metallic substrate. Simultaneously carbides were injected into the melt pool just behind the laser beam and shielded with argon gas flowing at 4 l/min. The powders were injected at the rate of 2 g/min.

3. RESULTS AND DISCUSSION

3.1 Microstructural Characterization

3.1.1 304L reinforced with TiC

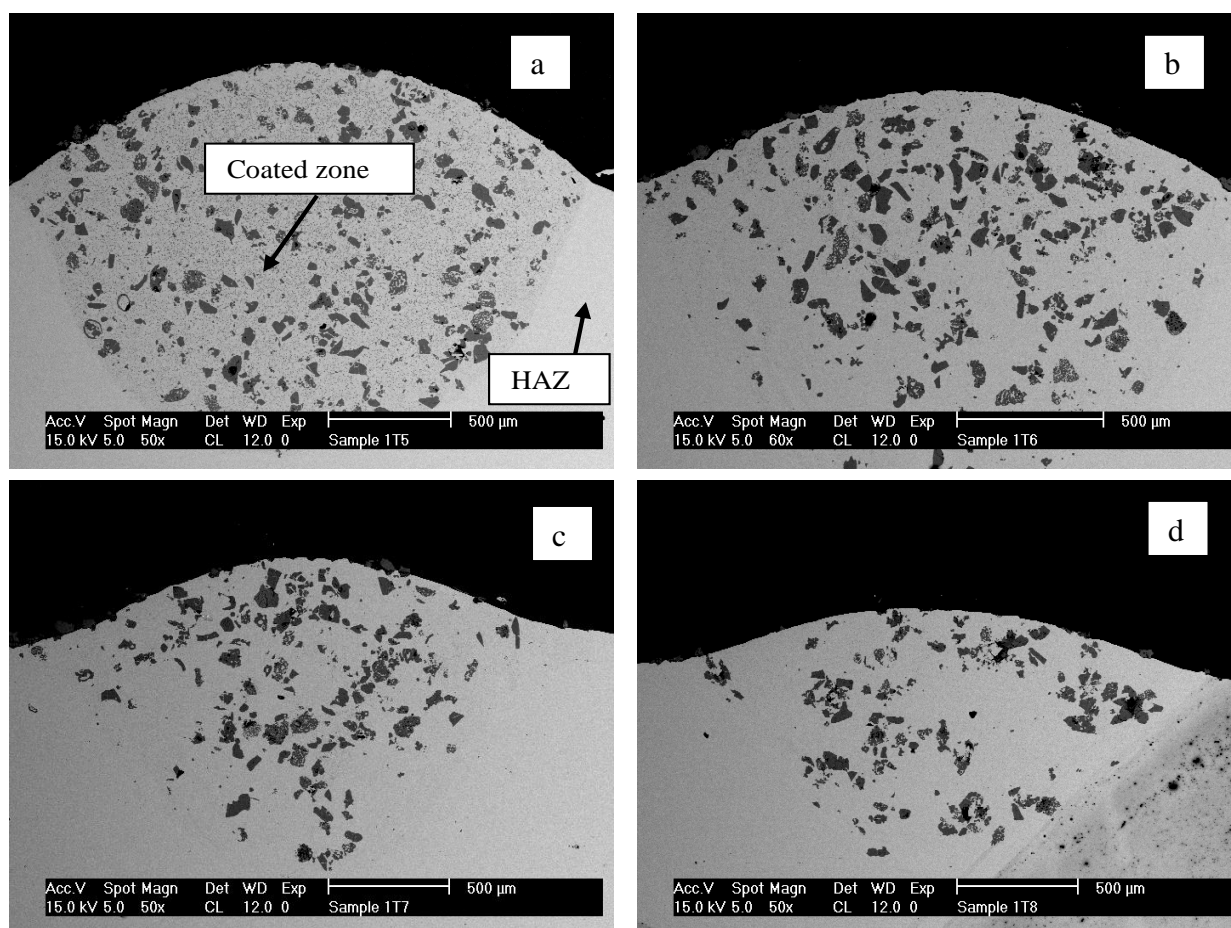


Figure 2. SEM images of TiC reinforced 304L ASS multiple tracks at power of 2.0 kW and scan speed of (a) 0.6 (b) 0.8 (c) 1.0 and (d) 1.2 m/min.

Fig. 2 shows the SEM images of the cross section of 304L ASS specimen after LMI process. It was observed that laser power and scan speeds affect the sizes and morphologies of the deposited

particulates. When the scan speed was varied from 0.6 to 1.2 m/min, the volume of particulates deposited increased with uniform distribution in the melt pool. When the laser beam was scanned over the substrate, energy was directly absorbed from the laser by the solid particles through both bulk coupling and powder coupling mechanisms [11].

It was also seen that, the faster the scan speed of the beam, the smaller the volume and mass of particulates deposited. Examination of the SEM micrographs of the samples revealed that the volume fraction of the TiC particles in the 304L ASS lessens with faster scan speed which points to the fact that the scan speed is inversely proportional to the energy input, consequently a lower interaction time.

The homogeneous distribution could be attributed to strong marangoni convection in the melt pool [12-13]. The different microstructures observed can be related to the variation in the thermodynamic and kinetic characteristics, such as solid-liquid wettability and continuous particle circulation during laser melting. At a suitable laser power of 2.0 kW and scanning speed of 0.6 m/min a sufficient amount of liquid phase is generated and this favours the distribution of TiC particles in the melt pool, thus a homogeneous distribution of the reinforcement in the matrix as shown in the SEM images in Figure 2a was obtained.

3.1.2 304L reinforced with WC-9Co-4Cr

Fig. 3 shows the SEM micrographs of the 304L specimen reinforced with WC-9Co-4Cr at laser power of 2.0 kW and varying scan speeds of 0.6 to 1.2 m/min. No pores and cracks were present as seen from the SEM images. It can be seen that undissolved WC cermets are present at the top surface of the coatings and this vary for all coatings, with specimen 1 alloyed at laser power of 2.0 kW and scan speed of 0.6 m/min having most of such undissolved carbides. This can be attributed to the volume of carbides injected, the fast scan speed and the coated surface exposure to the environment. At low scan speeds, more carbides were injected into the melt pool and due to high cooling rate, the carbides at the top solidifies before being dissolved. High wettability of WC and strong marangoni convection also aids the uniform distribution of dissolved carbides in the melt pool and segregation of the undissolved carbides at the coatings surfaces.

The volume fraction of deposited unmelted WC also seems much more on the coating injected at lowest scan speed for instance sample injected at 0.6 m/min, showed a high level of WC segregation coupled with a high depth and width of the injected zone. The effect of segregation on the investigated properties should be clear after analysis. The segregation of impurities and alloying elements during solidification is called coring or macrosegregation and may result in variation in the properties of material across the injected zone; it creates regions of flaw within this zone. Conclusion can be made that the LMI parameters used actually controlled the width of the melt pool, the quantity of powder injected into it and hence the properties so modified, this can simply be because of the longer lifetime of the melt pool which allows for more injection of the powder.

Melting, dissolution and resolidification of WC took place to form WC, W_2C , Co_6W_6C and $M_{23}C_6$ (M=Fe, Cr, W) as indicated by the XRD analysis obtained.

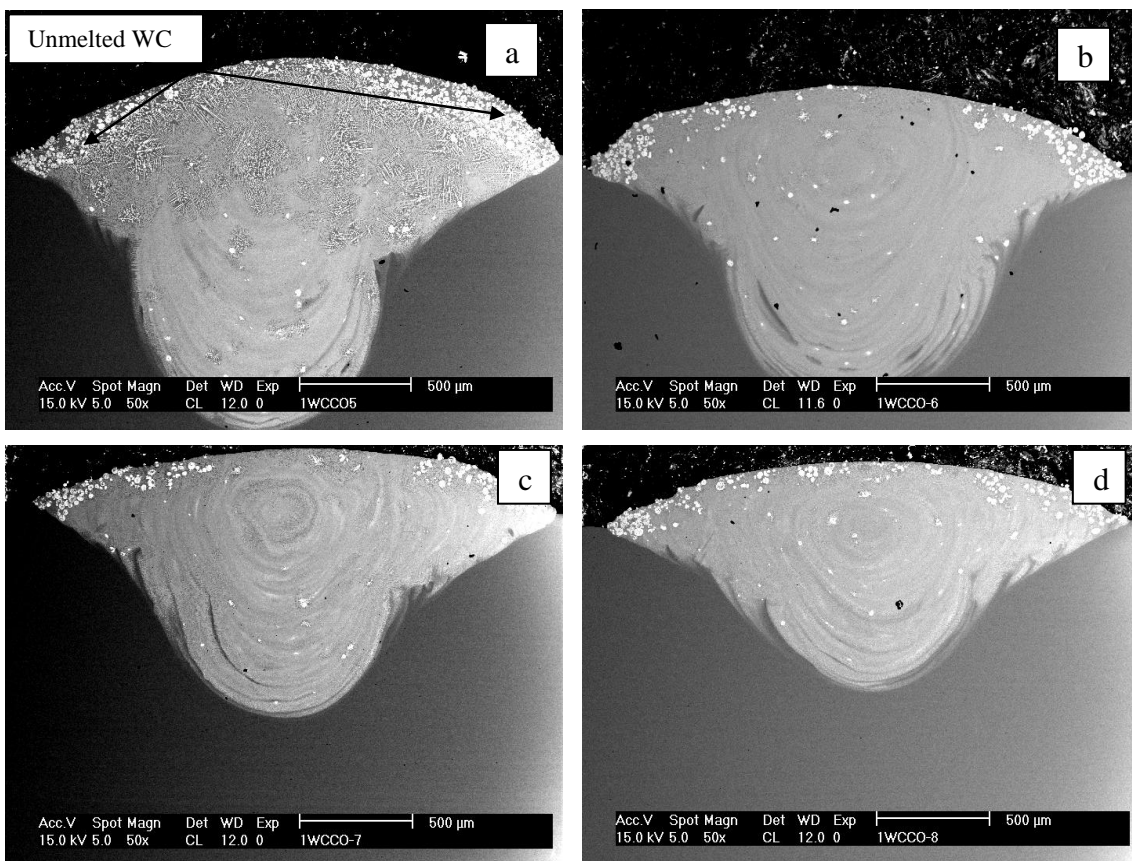


Figure 3. SEM images of 304L ASS reinforced with WC-9Co-4Cr at laser power of 2.0 kW and scan speed of (a) 0.6 (b) 0.8 (c) 1.0 and (d) 1.2 m/min.

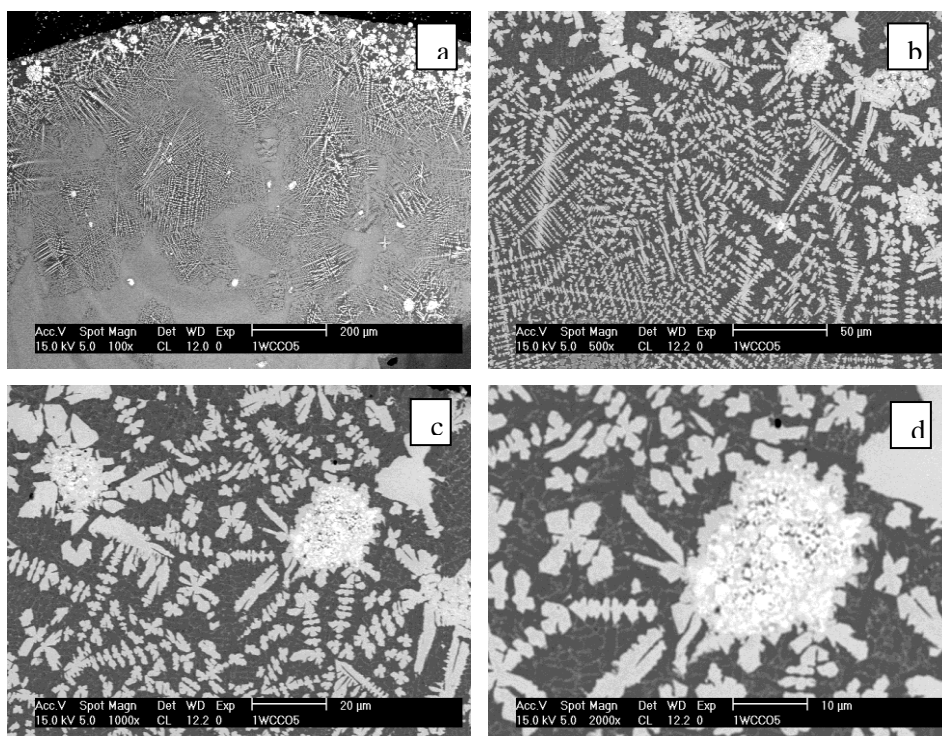


Figure 4. High magnification SEM micrograph of 304L reinforced with WC-9Co-4Cr showing dendrites

Fig. 4 shows the higher magnification SEM micrographs of WC-9Co-4Cr in the matrix of 304L ASS. The presence of large faceted primary carbide dendrites could be seen. The faceted carbide dendrites grow on the particle surface and propagate deep into the melt pool (Fig. 4a and b). Segregation of the carbides is also observed clearly. According to [14] the observed structure demonstrates that the growth of primary faceted carbide dendrites under conditions of high supersaturation is able to continue in the liquid that would not support it under the conditions close to equilibrium.

3.1.3 304L reinforced with WC-9Co-4Cr+TiC

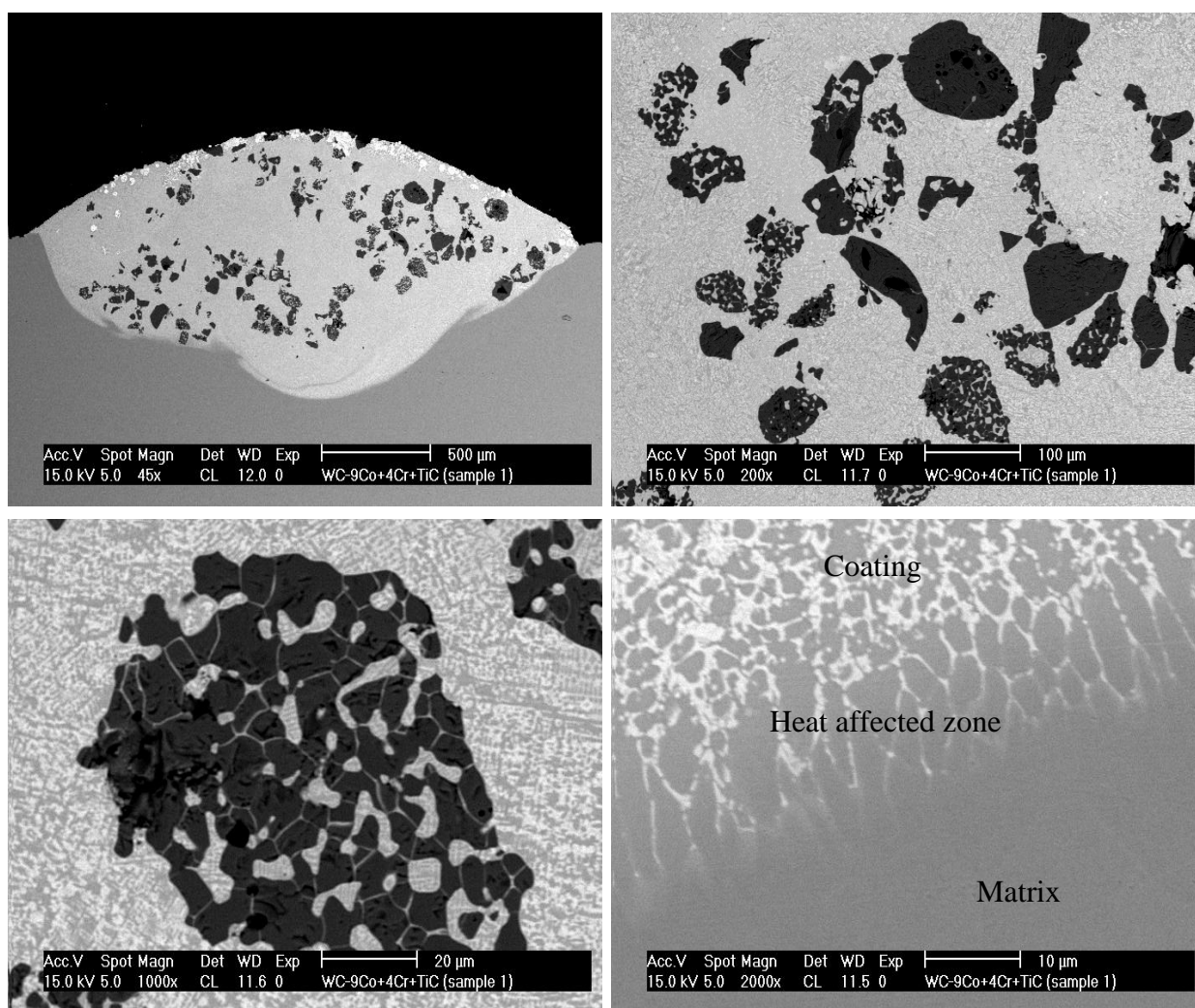


Figure 5. SEM images of 304L ASS reinforced with WC-9Co-4Cr+TiC at laser power of 2.0 kW and scan speed of 0.6 m/min.

The microstructures of laser melt injected TiC/WC-9Co-4Cr reinforced 304L ASS sample is shown in Figure 5. At 30% addition of TiC to WC cermet using the same laser parameters (laser power of 2.0 kW and scan speed of 0.6 m/min), the microstructure of the coating changed with most of the

TiC particles found in the middle zone of the coating. Also, the depth of coating has been drastically reduced when compared to Figure 3a. This could be attributed to the influence and volume fraction of TiC present in the melt pool.

The volume of TiC and the alloying elements within the matrix of the substrate such as chromium and silicon form very hard-high temperature resistance carbides and according to [15] limited further melting of the substrate since the rate of under-cooling in the area of the carbide particles were higher and far away from them. As a result, substrate containing low carbide formers (chromium, silicon, titanium) usually form large melt pool compared to substrates containing more carbide formers in this case WC and TiC.

3.2 EDS and XRD Analyses

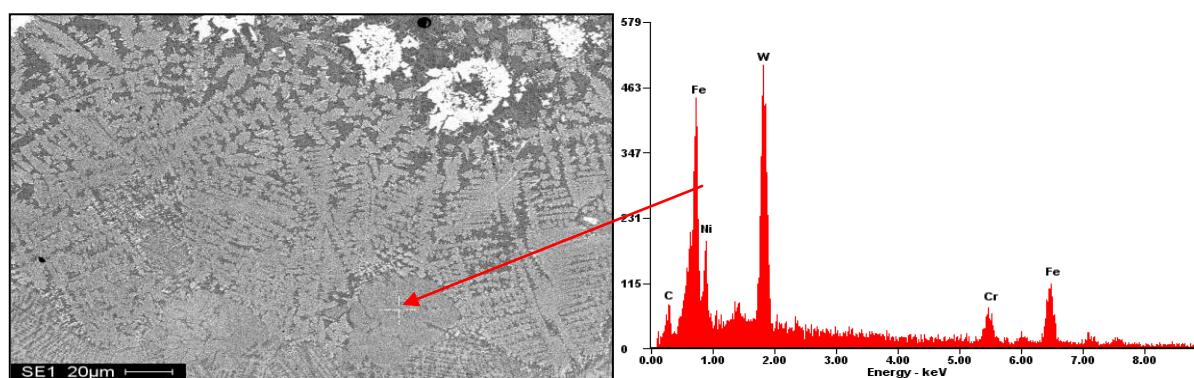


Figure 6. EDS analysis of 304L austenitic stainless steel reinforced with WC-9Co-4Cr at laser power of 2 kW and speed of 0.6 m/min.

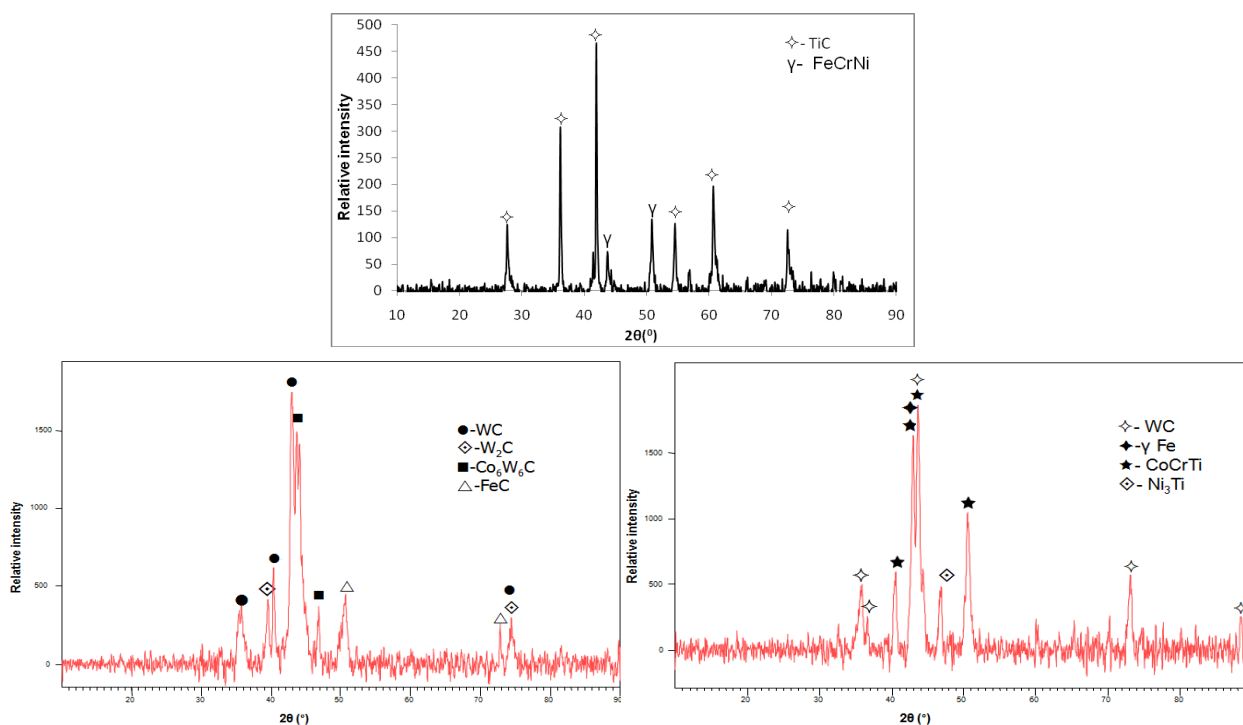


Figure 7. XRD analysis of (a) 304L+TiC (b) 304L+WC-9Co-4Cr and (c) 304L+WC-9Co-4Cr+TiC

3.3 Hardness and Depth Measurement

EDS analysis of the coated zone is shown in Fig. 6. Point analysis indicates the presence of high Fe and W content in the coatings. This could be due to WC high wettability in the melt pool. XRD analysis in Fig. 7 confirms the formation of suitable phases that are not detrimental to the properties of the composite compared to the single powders with no TiC addition.

The microhardness profile of the sample is shown in Fig. 8. Because of the reinforced effect of the WC and TiC and the intermetallics precipitated in the matrix, the microhardness of coated layer for WC-9Co-4Cr (average $Hv_{0.1}$ 1064) and WC-9Co-4Cr+TiC (average $Hv_{0.1}$ 1016) are higher than that of the substrate 304L ASS ($Hv_{0.1}$ 236).

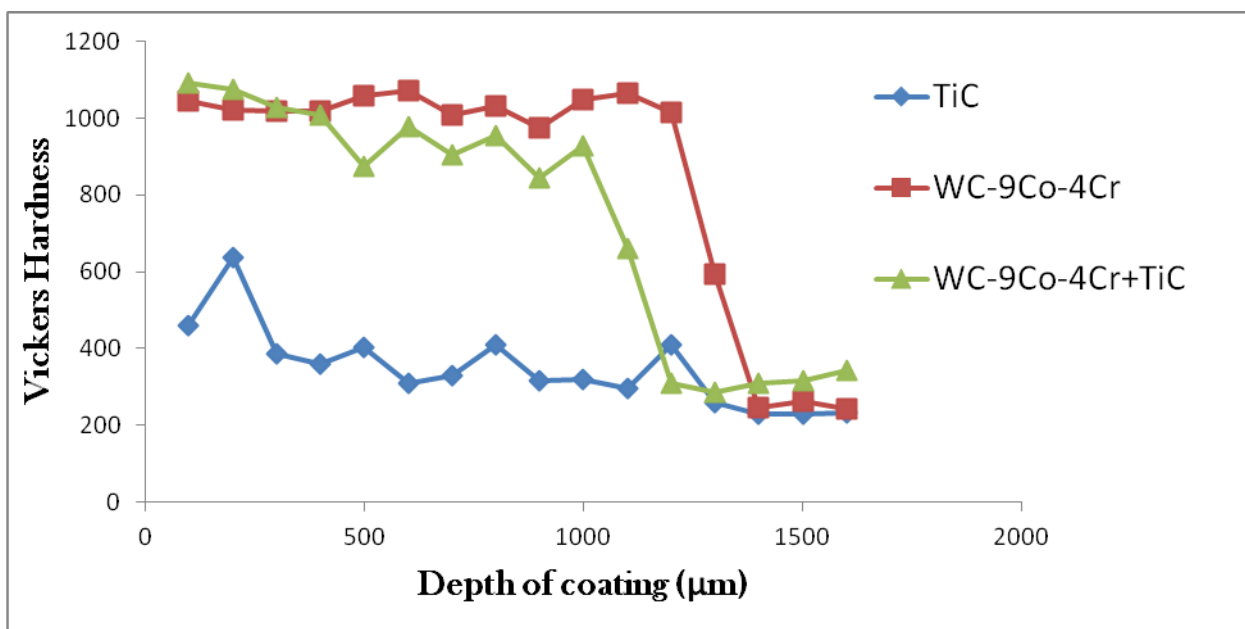


Figure 8. Microhardness measurement of laser treated 304L ASS.

The coating depth varies for all the coatings produced. Coating with the highest volume of carbides (WC-9Co-4Cr+TiC, 1270 µm) has the lowest coating depth compared to the WC-9Co-4Cr 1380 µm. The hard high temperature resistance carbide (WC-TiC) limited further melting of the substrate. It can be concluded that the hardening using WC-9Co-4Cr+TiC powder is due to the formation of MMC which is as a result of the dispersion of the hard particles EDS analysis showed the presence of large quantity of undissolved WC in the matrix, which resulted in solution strengthening, grain size refinement and enhancement of the hardness of the matrix. TiC, as reinforcement, improves the mechanical properties at room and high temperatures. TiC is very hard, is wear resistance and has a good wettability in the iron melt. In WC-Co/Cr systems, WC offers very high hardness, the cobalt acts as good binder while Cr offers high corrosion resistance due to their abilities to form stable and protective surface films.

3.4 Corrosion Measurement

The comparative corrosion behaviour of the substrate and the composites (TiC, WC cermet) was studied in 3.5% NaCl at room temperature. The corrosion results obtained from the electrochemical tests at room temperature are shown in Table 2. Figure 8 represent the potentiodynamic polarization curves of as-received and laser melt injected samples.

Table 2. Electrochemical test data obtained from polarization curves for samples laser injected at 2 kW power and 0.6 m/min scan speed.

Sample Labels	Laser Power/ Scan Speed (kW/m min ⁻¹)	Specimen	E_{corr} (V _{sce})	I_{corr} (A/cm ²)	Polarisation Resistance (Ω)	Corrosion Rate (mm/y)
0	2/0.6	304L	-0.79	1.1x10 ⁻⁷	4.63x10 ³	1.4x10 ⁻³
1	2/0.6	TiC	-0.92	1.5x10 ⁻⁸	1.51x10 ³	5.7x10 ⁻²
2	2/0.6	WC-9Co-4Cr	-0.90	2.9x10 ⁻⁸	1.14x10 ³	2.9x10 ⁻³
3	2/0.6	WC-9Co-4Cr+TiC	-0.87	2.4x10 ⁻⁹	1.89x10 ⁴	3.6x10 ⁻³

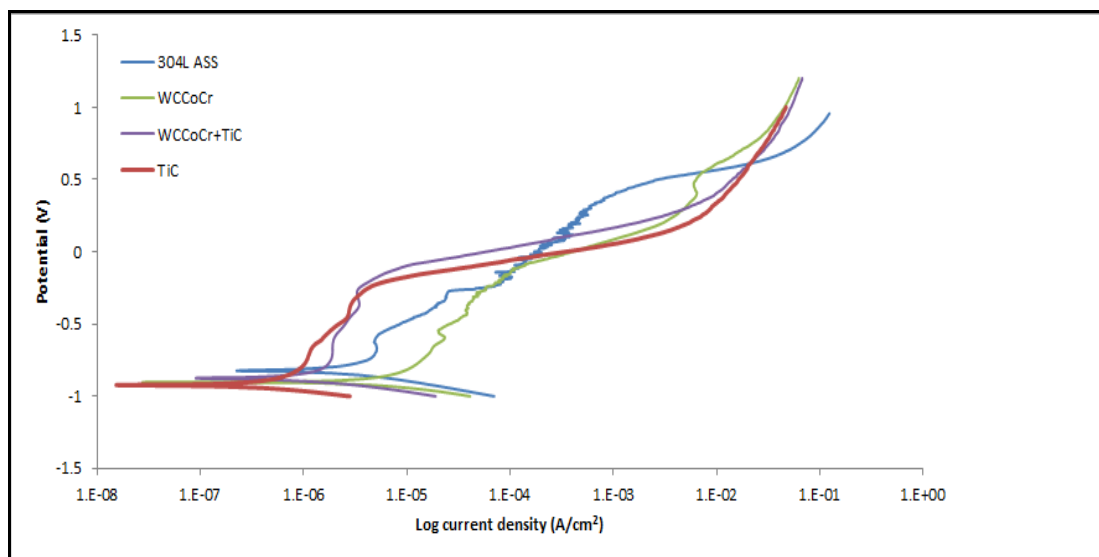


Figure 8. Polarization curves of studied as-received and laser treated samples of 304L ASS exposed to 3.5% NaCl solution (potential scanning rate: 0.2 mV/S).

Based on corrosion potential values recorded alone the 304L ASS is still the most corrosion resistant amongst all samples evaluated, it exhibits the most positive E_{corr} of -0.79 V. From the polarization curve, it is seen that TiC reinforced 304L steel shows the most negative E_{corr} of -0.92 V compared to other coatings; the layer behaves more actively in the solution. On the basis of corrosion potential values recorded alone; this coating is the least corrosion resistant. The homogeneous distribution of the reinforcement and lack of flaws and segregation in the TiC coating is supposed to favour high corrosion resistivity, but this is not so. Moreover, the phases revealed by XRD for this

coating are TiC and FeCrNi. Most of TiC particles did not dissolve but were uniformly distributed within the ASS matrix, while intermetallic FeCrNi has very small constituent as evidenced by the XRD peaks. This behaviour can be attributed to large volume fraction of TiC in the 304L ASS matrix. The influence of carbon on iron is evident, carbon dissolution in iron does not promote good corrosion behaviour but it is still advantageous in that it has positive effect on other properties such as hardness; and that is why during the manufacture of stainless steels generally, carbon is reduced to ultra low levels. The WC-9Co-4Cr reinforced 304L steel displayed E_{corr} of -0.90 V. This behaviour is however not surprising because SEM analysis indicates segregation of the WC on the top of the injected zone. Corrosion property is very sensitive to any form of inhomogeneity and segregation. Corrosion attack leading to this high potential value in the laser treated WC-9Co-4Cr reinforced 304L steel may possibly be mainly confined to isolated regions which are likely to be areas of inhomogeneity, these areas could not provide adequate barrier to retard chloride ions entrance onto the matrix of the substrate. XRD analysis confirmed the formation of four phases WC, W_2C , Co_6W_6C and FeC in this coating. Corrosion reactions could be initiated at areas in the inner region where WC is the principal phase and thus affects W_2C . Results for this coating showed a low amount of Co_6W_6C and W metal. Nevertheless, WC-9Co-4Cr+TiC reinforced steel displayed E_{corr} of -0.87 V becoming more positive when the two reinforcements were combined. This E_{corr} value is however more positive than the corrosion potential recorded for the two single reinforcement coatings. The E_{corr} value was brought down by 0.03 to 0.05 V. XRD for this coating identified WC, γ Fe, CoCrTi, and Ni_3Ti . Ni_3Ti is a binary intermetallic compound displaying excellent stability (thermal and microstructural). It is well known as strengthening compound. Combination of titanium and nickel will be highly corrosion resistant; nickel is known to have high corrosion resistance in most environments and also the passive oxide films formed by titanium retards corrosion initiation and propagation strongly. Hence, the slightly positive shift in the E_{corr} value.

Similarly, from experimental results it is seen that the current density and the corrosion rate displayed by all the tested samples are in the same range except for the WC-9Co-4Cr+TiC reinforced 304L steel which shows lower values for these two (one order decrease in magnitude) than others. In the same way the polarization resistance for this coating is also one order higher in magnitude than other coatings. The difference in corrosion parameters values recorded between that of the coating demonstrating least corrosion resistance and the substrate are thus: corrosion potential of coatings are more negative than the substrate with about -0.13 V E_{corr} at maximum; I_{corr} of all the coatings are less than that of the substrate; R_p of all coatings seems to fall within the same range; and so is the corrosion rate. The substrate can only be said to be better than the coatings when E_{corr} value only is considered. However, if the differences in recorded values for all other parameters for both substrate and coatings are considered, they all exhibit approximately same magnitude. This simply points to the fact that all carbide coated 304L ASS can exhibit stable corrosion resistance in chloride solution. The hardness and other interrelated properties of 304L ASS can be modified by LMI without deterioration of its good corrosion behaviour; and specifically at certain optimized laser processing parameters where good dispersion, lack of heterogeneity, no distortion, and minimal or no segregation occurs. The coated specimens exhibited current that increases as the potentials increases meaning the systems are pseudo-passive in character. This pseudo-passive behaviour could be as a result of carbides precipitates

occurring alongside a discontinuous layer of Cr on the coating surface forming a weak discontinuous chromium oxide/hydroxide passive layer. According to [16] some amount of Cr at the surface of the coatings could be tied up in carbides and less would be left in solid solution to form a continuous passive film on the specimen surface.

Galvanic corrosion cannot be disregarded. As reported by Wu et al. [7] and also confirmed by Falcon et al. [8], it is possible that galvanic corrosion cell may have been present in the locality of TiC particles in which case TiC could influence the development of many Cr-rich carbides and each Cr-rich carbide phase is a cause of exhaustion of valuable alloying element Cr, thereby leading to disintegration of their protective films and hence corrosion initiation and propagation. Slight galvanic corrosion took place [1] in the vicinities of the carbides reinforcements within the matrix but there is no case of complete degradation of the oxide coatings hence propagation of corrosion reactions did not occur. According to polarization data all parameters measure are similar in magnitude, hence corrosion property is stable.

4. CONCLUSIONS

❖ It has been demonstrated that laser melt injection can be used to obtain coatings on 304L ASS material.

❖ The degree of powder injection can be varied by changing the beam power, the beam travel velocity and the powder injection rate.

❖ A relationship has been established between the degree of particle injection and microstructure displayed by coating, microhardness and corrosion resistance.

❖ The microhardness reaches a maximum of 1064 $H_{V0.1}$ for WC-9Co-4Cr and 1016 $H_{V0.1}$ for WC-9Co-4Cr+TiC reinforced 304L austenitic stainless steel compared to the as-received 236 $H_{V0.1}$ - which is approximately 5 times that of the substrate.

❖ The corrosion resistance of all the coatings were approximately in the same range; complete deterioration of corrosion properties was not recorded. Stable corrosion behaviour was featured by approximately no change in values of corrosion current density, polarization resistance and corrosion rate for all coatings except for TiC reinforced coating. Amongst the coatings developed the WC-9Co-4Cr+TiC reinforced coating exhibited best corrosion resistance.

❖ The optimized laser processing parameters for high hardness and stable corrosion properties is Laser power of 2 kW; Scan speed of 0.6 m/min and injected powder feed rate of 2 g/min.

ACKNOWLEDGEMENT

This material is based upon work supported financially by the National Research Foundation. The National Laser Centre, CSIR, Pretoria is appreciated for laser facility. Babatunde Obadele, Research assistant and D Tech student of Tshwane University of Technology is fondly acknowledged.

References

1. A.P.I. Popoola, B.A. Obadele and O.M. Popoola, *Dig. J. Nanomater., Bios* 7 (2012) 1245.
2. W. Li, *J. Southeast University*, 20 (2004) 846.

3. J.D. Majumdar, B.R. Chandra and I. Manna, *Tribol. Int.*, 40 (2007) 146.
4. D. Liu, L. Li, F. Li and Y. Chen, *Sur. Coat. Tech.*, 202 (2008) 1771.
5. I.Y. Khalfallah, M.N. Rahoma, J.H. Abboud and K.Y. Benyounis, *Opt. Laser Technol.*, 43 (2011) 806.
6. A.P.I. Popoola, S.L. Pityana and O.M. Popoola, *SAIMM.*, 111 (2011) 345.
7. Q. Wu, W. Li and N. Zhong, *Corros. Sci.*, 53 (2011) 4258.
8. L.A. Falcon, E.B. Bedolla, J. Lemus, C. Leon, I. Rosales and J.G. Gonzalez-Rodriguez, *Int. J. Corros.*, (2011) 1.
9. G. Thawari, G. Sundararajan and S.V. Joshi, *Thin Solid Films*, 423 (2003) 41.
10. S.L. Pityana, *Proceedings of the fifth international WLT-conference on lasers in manufacturing*, June 15-18 (2009) Munich, Germany.
11. P. Fischer, V. Romano, H.P. Weber, N.P. Karapatis, E. Boillat and R. Glardon, *Acta Mater.*, 51 (2003) 1651.
12. C. Tassin, F. Laroudie, M. Pons and L. Lelait, *Sur. Coat. Tech.*, 76 (1995) 450.
13. O. Verezub, Z. Kálazi, G. Buza, N.V. Verezub and G. Kaptay, *Sur. Coat. Tech.*, 203 (2009) 3049.
14. M. Riabkina-Fisherman, E. Rabkin, P. Levin, W. Frage, M.P. Darel, A. Weisheit, R. Galin and B.L. Mordike, *Mater. Sci. Eng.*, A302 (2001) 106.
15. Q. Li, T.C. Lei and W.Z. Chen, *Sur. Coat. Tech.*, 114 (1999) 278.
16. C.T. Kwok, K.H. Lo, F.T. Cheng and H.C. Man, *Sur. Coat. Tech.*, 166 (2003) 221.